

Enhanced Algorithms for EO/IR Electronic Stabilization, Clutter Suppression, and Track-Before-Detect for Multiple Low Observable Targets

Alexander G. Tartakovsky

*Argo Science Corp. and University of Southern California
Los Angeles, CA*

Andrew P. Brown

*Toyon Research Corporation
Goleta, CA*

James Brown

*Air Force Research Laboratory/VSBYB
Hanscom AFB, MA*

ABSTRACT

We develop and evaluate a suite of advanced algorithms which provide significantly-improved capabilities for finding, fixing, and tracking multiple ballistic and flying low observable objects in highly stressing cluttered environments. The algorithms have been developed for use in satellite-based staring and scanning optical surveillance suites for applications including theatre and intercontinental ballistic missile early warning, trajectory prediction, and multi-sensor track handoff for midcourse discrimination and intercept. The system performs sensor motion compensation providing sub-pixel stabilization (to 1/100 of a pixel), as well as advanced spatial-temporal clutter estimation and suppression to below sensor noise levels, followed by statistical background modeling and nonlinear Bayesian multiple-target track-before-detect filtering. The multiple-target tracking is performed in physical world coordinates to allow for multi-sensor fusion, trajectory prediction, and intercept. The algorithms are designed to handle a wide variety of real-world challenges: the scene background may contain significant celestial, earth limb, or terrestrial clutter, and the targets of interest may be dim, relative to the scene background. The performance of the developed algorithms is demonstrated using real-world data containing resident space objects observed from the MSX platform, with backgrounds varying from celestial to combined celestial and earth limb. Simulation results are also presented for parameterized variations in signal-to-clutter levels (down to 1/1000) and signal-to-noise levels (down to 1/6) for simulated targets against real-world terrestrial clutter backgrounds.

1. INTRODUCTION

The problem of efficient detection and tracking of multiple dim targets is a challenge for space-based IR/EO sensors. In fact, in the raw image sequence the signal-to-clutter ratio (SCR) may be as low as 10^{-3} , in which case detection and tracking without preliminary spatial-temporal image processing and clutter rejection is almost impossible. For geostationary sensors, this problem has been partially solved by Tartakovsky and Brown [4]. As has been shown in this work, the excess false alarm problem can be addressed only through sophisticated spatial-temporal image processing for clutter rejection (CLUR). Specifically, conventional spatial and differencing methods are not sufficient, and advanced spatial-temporal CLUR filters are required. One of the major nuisance factors (even for mechanically stabilized IR/EO sensors and geostationary platforms) that prevents efficient temporal processing is LOS (line-of-sight) non-regular and uncontrollable changes due to vibration, which results in translational and rotational image distortions. Existing mechanical methods of sensor stabilization are very expensive and are not efficient enough, as was demonstrated in [4].

This paper focuses on the development and evaluation of a suite of advanced algorithms which provide significantly-improved capabilities for finding, fixing, and tracking multiple ballistic and flying low observable objects in highly stressing cluttered environments. The algorithms have been developed for use in satellite-based staring and scanning optical surveillance suites for applications including theatre and intercontinental ballistic missile early warning, trajectory prediction, and multi-sensor track handoff for midcourse discrimination and intercept. As illustrated in Figure 1,

Address correspondence to A. G. Tartakovsky, Argo Science Corp., 71 Cypress Way, Rolling Hills Estates, CA 90274; E-mail: tartakov@argoscience.com or A. P. Brown, Toyon Research Corporation, 6800 Cortona Drive, Goleta, CA 93117; E-mail: abrown@toyon.com

the functions performed by the algorithms include sensor motion (and/or platform vibration) compensation, providing sub-pixel stabilization (to 1/100 of a pixel), advanced spatial-temporal clutter estimation and suppression to below sensor noise levels, statistical background modeling, and Bayesian nonlinear multiple-target track-before-detect filtering. The multiple-target tracking is performed in physical world coordinates to allow for multi-sensor fusion, trajectory prediction, and intercept. Output of detected object cues and data visualization are also provided.

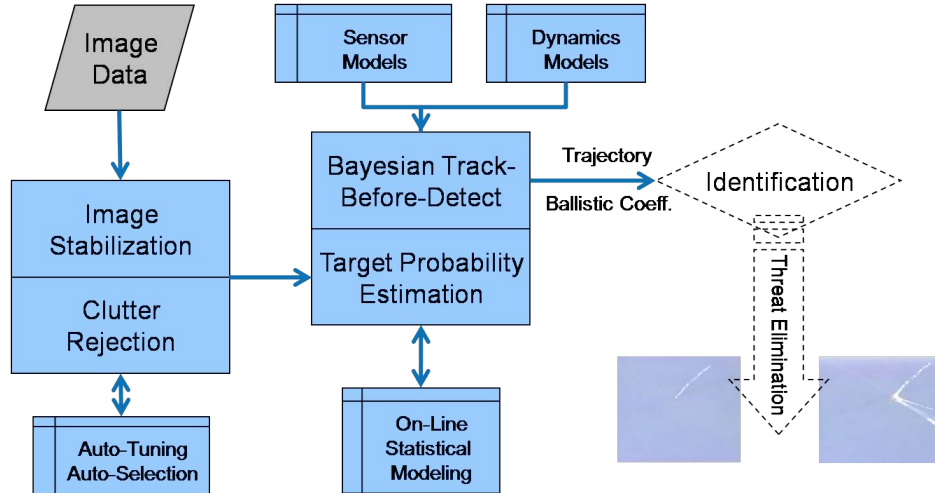


Figure 1. Block diagram illustrating functionality of the enhanced low observables algorithms.

The algorithms are designed to handle a wide variety of real-world challenges. Sequences of images may be highly complex and infinitely varied—the scene background may contain significant celestial, earth limb, or terrestrial clutter. For example, when viewing combined earth limb and terrestrial scenes, a combination of stationary and non-stationary clutter may be present, including cloud formations, varying atmospheric transmittance and reflectance of sunlight and other celestial light sources, aurora, glint off sea surfaces, and varied natural and man-made terrain features. The targets of interest may be (and usually are) dim, relative to the scene background, rendering much of the existing deployed software useless for optical target detection and tracking. Additionally, it may be necessary to detect and track a large number of objects in the threat cloud, and these objects may not always be resolvable in individual data frames.

The performance of the developed algorithms is demonstrated using real-world data containing resident space objects observed from the MSX platform, with backgrounds varying from celestial to combined celestial and earth limb. Simulation results are also presented for parameterized variations in signal-to-clutter levels (down to 1/1000) and signal-to-noise levels (down to 1/6) for simulated targets against real-world terrestrial clutter backgrounds. We also discuss algorithm processing requirements and software processing capabilities from our on-going development of an image processing toolkit (iPTK).

The rest of the paper is organized as follows. In Section 2, we outline the developed CLUR methods for geostationary platforms, and illustrate that this development is indeed important by comparing with the typical state-of-practice differencing methods. Section 3 is devoted to the clutter suppression issues for highly non-stationary conditions that arise in scenarios where sensors are situated on moving platforms such as low Earth orbit (LEO) satellites, highly elliptical orbit (HEO) satellites (high Earth orbits), etc. In Section 4, we outline our non-linear track-before-detect algorithm, and we provide example results in stressing cases, including tracking objects with dramatically different velocities and intensities in MSX SBV data, and 3D coordinate tracking of an extremely dim simulated ballistic target against a EUMETSAT clutter background. Finally, in Section 5 we draw conclusions and make final remarks.

2. CLUTTER REJECTION FOR GEOSTATIONARY SENSORS

In a geostationary scenario, the developed baseline CLUR technique is based on a multi-parametric approximation of clutter that leads to an adaptive spatial-temporal filter. The results of an extensive experimental study [4] show that the proposed algorithm gives a substantial gain compared to the best existing spatial techniques as well as to the industry standard temporal differencing method.

We observe a sequence of $N_x \times N_y$ IR images (intensities) that have the form

$$I_n(\mathbf{r}_{ij}) = \sum_{k=1}^{K_n} A_n(k)S(\mathbf{r}_{ij} - \mathbf{r}_n(k) - \boldsymbol{\delta}_n) + b_n(\mathbf{r}_{ij} - \boldsymbol{\delta}_n) + \xi_n(\mathbf{r}_{ij}), \quad n = 1, 2, \dots, \quad (1)$$

where $\xi_n(\mathbf{r}_{ij})$ is sensor noise; $b(\mathbf{r}_{ij})$ is clutter (background); $A_n(k)S(\mathbf{r}_{ij} - \mathbf{r}_n(k))$ is a signal from the k -th target with spatial coordinates $\mathbf{r}_n(k) = (X_n(k), Y_n(k))$ and maximal intensity $A_n(k)$; $S(\mathbf{r}_{ij})$ is the target signature related to the sensor's point spread function (PSF); K_n is an unknown number of targets in the n -th frame; $\boldsymbol{\delta}_n = (\delta_x(n), \delta_y(n))$ is an unknown 2D shift due to the jitter (LOS vibrations); $\mathbf{r}_{ij} = (x_i, y_j)$ is the pixel in the plain image with coordinates (x_i, y_j) , $i = 1, \dots, N_x$, $j = 1, \dots, N_y$.

We will use boldface for a vector/matrix notation, e.g., $\mathbf{I}_n = \{I_n(\mathbf{r}_{ij}), i = 1, \dots, N_x, j = 1, \dots, N_y\}$.

The goal is to build a spatial-temporal filter that rejects clutter as much as possible and simultaneously compensates for the jitter (stabilizes the scene), while preserving signals from targets as much as possible.

We consider residual-type filtering algorithms of the form $\tilde{I}_n(\mathbf{r}_{ij}) = I_n(\mathbf{r}_{ij}) - \hat{b}_n(\mathbf{r}_{ij})$, where $\tilde{I}_n(\mathbf{r}_{ij})$ is the output of the filter and $\hat{b}_n(\mathbf{r}_{ij})$ is an estimate of clutter $b_n(\mathbf{r}_{ij})$ in the pixel (i, j) of the current n -th frame based on the previous frames $I_{n-m+1}(\mathbf{r}_{ij}), \dots, I_n(\mathbf{r}_{ij})$ in a sliding window of the size m ($n \geq m$).

We assume that in the time interval of m frames the function $b_n(\mathbf{r})$ is slowly varying, i.e., we can neglect changes due to physical causes such as wind, illumination conditions, temperature, convection, etc. Under this assumption, the clutter function $b_n(\mathbf{r}_{ij})$ changes in time in each pixel only because of the sensor vibrations (locally within a certain time interval).

The proposed CLUR algorithms are adaptive and robust (use minimum prior information regarding the statistical properties of clutter and jitter). We suppose that translations $\boldsymbol{\delta}_n$ are arbitrary unknown variables bounded by a maximum possible amplitude of the sensor vibrations and $b_n(\mathbf{r})$ is an arbitrary unknown non-negative function with a bounded spatial band, slowly changing in time. In the geostationary staring IR sensor scenario the value of $\boldsymbol{\delta}_n(\mathbf{r}) = \boldsymbol{\delta}_n$ is just the parallel shift that does not depend on \mathbf{r} .

The value of m defines the length of the interval in which clutter does not change substantially (slowly varying). Spatial-temporal filtering for clutter rejection is based on the data $(\mathbf{I}_{n-m+1}, \dots, \mathbf{I}_n)$ in the sliding window m .

2.1. Clutter Suppression. We now proceed with a description of the basic idea and a generic CLUR algorithm. Assume that the function $b_n(\mathbf{r})$ can be approximated by a parametric model

$$b_n(\mathbf{r}) \approx \sum_{k=1}^M \theta_k f_k(\mathbf{r}), \quad (2)$$

where θ_k are unknown parameters and $f_k(\mathbf{r})$ are given functions chosen from the best fitting criterion.

Let $\hat{\theta}_k(n)$ denote an estimate of θ_k based on the data $\mathbf{I}_{n-m+1}, \dots, \mathbf{I}_n$ in the time window $[n - m + 1, n]$ of the length m . According to (2), for any shift $\boldsymbol{\delta}$, the prediction estimate of the background at time n has the form:

$$\hat{b}_n(\mathbf{r} - \boldsymbol{\delta}) = \sum_{k=1}^M \hat{\theta}_k(n) f_k(\mathbf{r} - \boldsymbol{\delta}). \quad (3)$$

Assume that the shifts $\boldsymbol{\delta}_s$ are fixed (estimated) and let $\hat{\boldsymbol{\delta}}_s$ denote these estimates. Write

$$\mathcal{E}_n(\boldsymbol{\theta}, \{\hat{\boldsymbol{\delta}}_s\}) = \sum_{i=1}^{N_x} \sum_{j=1}^{N_y} \sum_{s=n-m+1}^n \left(I_s(\mathbf{r}_{ij}) - \sum_{k=1}^M \theta_k f_k(\mathbf{r}_{ij} - \hat{\boldsymbol{\delta}}_s) \right)^2.$$

The estimate $\hat{\boldsymbol{\theta}}_n$ is found from the least squares criterion:

$$\hat{\boldsymbol{\theta}}_n = \underset{\boldsymbol{\theta}}{\operatorname{argmin}} \mathcal{E}_n(\boldsymbol{\theta}, \{\hat{\boldsymbol{\delta}}_s\}). \quad (4)$$

The parameter estimation algorithm requires a reasonably accurate estimation of the shift $\boldsymbol{\delta}$, i.e., jitter compensation. This latter estimation/compensation can be done either by an independent jitter estimation algorithm or iteratively in the course of estimating parameters $\boldsymbol{\theta}$.

Suppose now that the estimate $\hat{b}_{n-1}(\mathbf{r})$ of the $(n-1)$ -st frame is already obtained. For jitter estimation in the n -th frame, we use the minimum distance estimate $\hat{\delta}_n = (\hat{\delta}_x(n), \hat{\delta}_y(n))$, which is the solution of the following *nonlinear* minimization problem:

$$\hat{\delta}_n = \underset{|\delta| \leq \delta_{\max}}{\operatorname{argmin}} \sum_{i=1}^{N_x} \sum_{j=1}^{N_y} \left(I_n(\mathbf{r}_{ij}) - \hat{b}_{n-1}(\mathbf{r}_{ij} - \delta) \right)^2. \quad (5)$$

We now summarize the generic CLUR method that uses an iterative procedure for jitter compensation (frame alignment) and the background estimation. The algorithm starts with initialization, which provides the pilot estimates $\hat{\theta}_k(m)$, $(\hat{\delta}_1, \dots, \hat{\delta}_m)$, and $\hat{b}_m(\mathbf{r}_{ij}) = \sum_{k=1}^M \hat{\theta}_k(m) f_k(\mathbf{r}_{ij} - \hat{\delta}_m)$. Initialization schemes include autonomous algorithms of estimation of shifts between two frames based on simple spline-approximations. After initialization a typical step of the algorithm includes the following operations:

1. Jitter Estimation. The estimate $\hat{b}_{n-1}(\mathbf{r}_{ij})$ obtained from the previous step is compared with the n -th frame and the estimate of jitter $\hat{\delta}_n$ is computed as the solution of the nonlinear optimization problem (5) with $\hat{b}_{n-1}(\mathbf{r}_{ij} - \delta) = \sum_{k=1}^M \hat{\theta}_k(n-1) f_k(\mathbf{r}_{ij} - \delta)$.

2. Estimation of Parameters. Having the estimates $\hat{\delta}_{n-m+1}, \dots, \hat{\delta}_n$, the estimates $\hat{\theta}_k(n)$ are computed for the n -th frame from the minimization problem (4). This recomputing in the corrected coordinate system is equivalent to frame alignment.

3. Clutter Estimation. Using the estimates obtained from (4) and (5), compute the estimate of $b_n(\mathbf{r}_{ij})$ for all i and j in the corrected coordinate system, i.e., $\hat{b}_n(\mathbf{r}_{ij}) = \sum_{k=1}^M \hat{\theta}_k(n) f_k(\mathbf{r}_{ij} - \hat{\delta}_n)$.

4. Clutter Rejection. Using the estimate $\hat{b}_n(\mathbf{r}_{ij})$ from the previous step, compute the residuals (filtered background)

$$\tilde{I}_n(\mathbf{r}_{ij}, \hat{\delta}_n) = I_n(\mathbf{r}_{ij}) - \sum_{k=1}^M \hat{\theta}_k(n) f_k(\mathbf{r}_{ij} - \hat{\delta}_n).$$

Different filters in the bank of CLUR filters correspond to different choices of the basis f . For example, we used Fourier basis, wavelets, and splines (cubic and bi-linear), as well as certain polynomial approximations. For further details we refer to [4].

2.2. Detection and Tracking. The processed data from the CLUR filter come to the Target Detection Block. The output of this block are the instantaneous detections (blips) with the estimates of the target positions and intensities. The in-frame detection algorithm realizes a generalized likelihood ratio hypothesis test with an adaptive threshold which stabilizes the false alarm rate and makes the density of false blips approximately uniform over the image.

The processed data from the output of the Target Detection Block come to the tracking system. The multitarget tracking scheme (including track management) is more or less standard in terms of the sequence of operations (see, e.g., [1]). However, the following important innovations are used: (1) global data association (optimal for association of all detections but not locally optimal for a particular detection); (2) adaptive selection of the polynomial power for current conditions through introduction of virtual tracks in the polynomial filter; and (3) optimal procedures for track initiation and termination based on changepoint detection methods (see [2, 3, 5]).

The tracker performs the following operations: (1) Identification/association of new detections (blips) with existing tracks; (2) Initiation of new tracks based on blips that are not identified as belonging to existing tracks; (3) Confirmation of newly initialized tracks; (4) Deletion of unconfirmed tracks; (5) Termination of tracks; (6) Dynamic correction of the information data base.

2.3. Efficiency Analysis. We now illustrate the efficiency of the developed methodology by comparing with the typical state-of-practice differencing method. The differencing CLUR method subtracts two consecutive frames.

We simulated an image sequence with moderately intense clutter and sensor noise standard deviation $\sigma_N = 3$. Two weak targets were inserted in the sequence. We first used the *Wavelet* spatial-temporal filter with window of $m = 20$ frames. The results were successful — the standard deviation of the residual clutter plus noise was about 3 and both targets were tracked, as can be seen in Figure 2(b). By contrast, with the differencing method we were not able to track targets, as seen from Figure 2(c). Squares with no tracks attached represent instantaneous detections part of which are false, while solid lines correspond to confirmed target tracks.

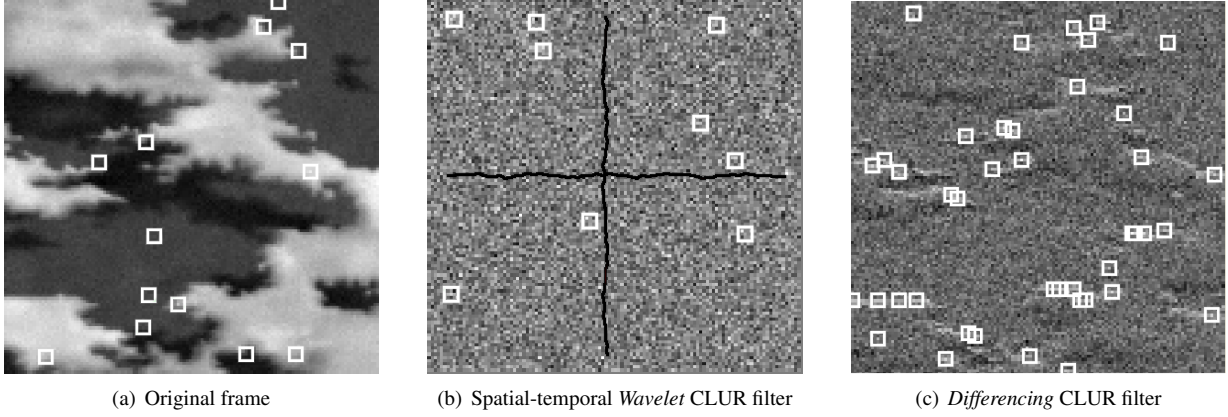


Figure 2. The results of target tracking using spatial-temporal Wavelet and differencing CLUR filters.

3. CLUTTER SUPPRESSION IN NONSTATIONARY CONDITIONS

While the clutter suppression method described in the previous section is very effective for geostationary staring sensors, it does not seem completely amenable to HEO (e.g., SBIRS-HIGH), LEO (e.g., STSS), and other non-stationary moving sensors. This method should be substantially modified to be efficient in non-stationary conditions. The CLUR algorithm should take into account the following specific features: (a) Nonstationarity related to sensor motion (not only translational and rotational stabilization is needed, but also image extrapolation, including compensation of perspective changes); (b) A three-dimensional cloud cover model; (c) Complexity of images.

The developed CLUR algorithm performs estimation of the projective transformation based on a linear approximation of the image intensity. This results in a system of 8 nonlinear equations solved by the Newton method. For estimation of large projection distortions, a multi-layer approach with Gaussian pyramids is used. The developed CLUR algorithm covers very general models with the images that are 3D-to-2D projections of a plane with an arbitrary orientation in 3D. The details of the algorithm are described below.

3.1. Estimation of the Projective Transformation. It is assumed that the intensity of the image in the vicinity of each pixel is described by the linear model:

$$I(x + dx, y + dy) = I(x, y) + \frac{\partial I}{\partial x} dx + \frac{\partial I}{\partial y} dy.$$

In order to find a transformation, we minimize a “loss” function that is given by the following quadratic norm:

$$\mathcal{L}_2 = \sum_{i,j} [I_0(i, j) - I(p_x(i, j), p_y(i, j))]^2 = \sum_{i,j} \left[I_0(i, j) - I(i, j) - \frac{\partial I}{\partial x} (p_x(i, j) - i) - \frac{\partial I}{\partial y} (p_y(i, j) - j) \right]^2 \quad (6)$$

where I_0 is the reference frame and I is the current frame.

Assume first that transformation leads to pixel shifts less than a pixel size, in which case

$$p_x(i, j) = \frac{c_0 i + c_1 j + c_2}{c_6 i + c_7 j + 1}, \quad p_y(i, j) = \frac{c_3 i + c_4 j + c_5}{c_6 i + c_7 j + 1}. \quad (7)$$

We now have to find the vector of coefficients $\mathbf{c} = (c_0, c_1, \dots, c_7)$. To this end, we substitute (7) in (6) and differentiate the resulting loss function over coefficients. The resulting derivatives $f_0(\mathbf{c}), f_1(\mathbf{c}), \dots, f_7(\mathbf{c})$ are equalized to zero, so that we obtain the system of eight nonlinear equations: $f_0(\mathbf{c}) = 0, f_1(\mathbf{c}) = 0, \dots, f_7(\mathbf{c}) = 0$, where

$$f_0(\mathbf{c}) = \sum_{i,j} \left(I_0(i, j) - I(i, j) + \frac{\partial I}{\partial x} i + \frac{\partial I}{\partial y} j - \frac{\partial I}{\partial x} \frac{c_0 i + c_1 j + c_2}{c_6 i + c_7 j + 1} - \frac{\partial I}{\partial y} \frac{c_3 i + c_4 j + c_5}{c_6 i + c_7 j + 1} \right) \frac{\partial I}{\partial x} \frac{i}{c_6 i + c_7 j + 1}.$$

For brevity’s sake we present only $f_0(\mathbf{c})$. The rest of the functions have an essentially similar form.

This system is solved iteratively by the Newton method. Specifically, let $\mathbf{W}(\mathbf{c}) = \|\partial f_k / \partial c_m\|$ be the Hessian of the loss function \mathcal{L}_2 and let $\mathbf{f}(\mathbf{c}) = (f_0(\mathbf{c}), f_1(\mathbf{c}), \dots, f_7(\mathbf{c}))$. The $(n + 1)$ -st step of the iterative method is given by

$$\hat{\mathbf{c}}_{n+1} = \hat{\mathbf{c}}_n - \mathbf{W}^{-1}(\hat{\mathbf{c}}_n)\mathbf{f}(\hat{\mathbf{c}}_n), \quad n = 0, 1, \dots$$

Recall that we assumed that shifts are smaller than a pixel size, which is not realistic for many scenarios of interest. In order to deal with shifts larger than a pixel, we use a Gaussian pyramid with twice smaller images. The previous procedure is used for estimation. The resulting matrix is scaled by two and is then used for image compensation at the next level of the pyramid with higher resolution. This process is repeated till the original resolution is achieved.

3.2. Clutter Estimation and Rejection. Let I_1, \dots, I_N be the batch of N sequential frames and let \mathbf{M}_{i+1} denote the matrix of the projective transformation between the $(i + 1)$ -st and i -th frames, so that $\mathbf{I}_{i+1} = \mathbf{M}_{i+1}\mathbf{I}_i$ for $i = 1, \dots, N - 1$. Clutter estimation is performed in the coordinate system of the last N -th frame. To this end, the matrices of the projective transformation are multiplied to obtain the final transformation (each-frame-to-the-last-frame):

$$\mathbf{M}_i^* = \mathbf{M}_i \times \mathbf{M}_{i+1} \times \dots \times \mathbf{M}_N.$$

After all matrices are determined, clutter is estimated for each pixel in the system of coordinate of the last image by the least squares method (LSM). For the quadratic model the corresponding system of equations is linear.

To be specific, let the background intensity around each pixel is approximated by the polynomial model

$$I(dx, dy) = C_0 + C_1dx + C_2dy + C_3dx^2 + C_4dy^2 + C_5dxdy.$$

where dx, dy are coordinates from the center of the output pixel. Then the LSM loss function is

$$\mathcal{L} = \sum_{i=1}^N (I_i - C_0 - C_1dx - C_2dy - C_3dx^2 - C_4dy^2 - C_5dxdy)^2. \quad (8)$$

More precisely, after all matrices are estimated the following sequence of operations is performed:

1. For each point (u, v) we find the closest point (u_i, v_i) in each frame in the batch in the window $m \times m$ (usually $m = 3$), using the estimated transformation matrices.
2. If the number of points is not sufficient, then the intensities are simply averaged.
3. The estimate of intensity in the current pixel is obtained from the solution of linear equations (LSM).

The third step needs a little more detailed explanation. Taking derivatives in (8) and equalizing to zero, we obtain the matrix equation for the coefficients C_0, \dots, C_5 . Note that we are primarily interested in the value of the constant C_0 that determines the intensity in the center of the pixel in the last frame. Solving this system, we find the estimate \hat{C}_0 , and then we subtract this value from the last frame, which yields the whitened frame (the output of the clutter rejection filter), i.e., $\tilde{I}_N = I_N - \hat{C}_0$.

3.3. Extraction of Blips and Tracking. For extraction of blips (detection) we use the simplest algorithm that performs thresholding of pixel intensities in whitened images. The threshold is calculated based on the following logic. First, a histogram of intensity distribution is calculated. Second, the histogram is integrated from small to large intensity values until the total number of pixels participating in the integration does not exceed the threshold level. For example, if the frame size is 512×512 and the probability is 10^{-4} , then the remaining number of pixels is $512 \times 512 \times 10^{-4} \approx 26$ the most intense pixels. These pixels produce blips. This approach allows for accounting of possible non-Gaussian character of the whitened frame related to residuals with clutter artifacts. Finally, the sub-pixel accuracy improvement of the estimates of blip locations is performed. To this end, in the 3×3 neighborhood of each blip the intensity is approximated with a parabola and its minimum is found.

Tracking is performed as described in Section 2.2.

3.4. Experimental Results. We performed a number of simulation experiments with semi-synthetic data. In the experiments targets are modeled as points that are mixed with the raw image prior to its processing. We used IR image sequences with real clutter (clouds, ground, and a combination thereof). Two orbits were considered: LEO and HEO.

Figure 3 shows the results of clutter rejection and target tracking for the highly non-stationary HEO MeteoSat data with the parameters: Perigee=500km; Apogee=35800 km; Input frame size 512×512 . It is seen that the original heavy cloud clutter has been almost completely removed which allowed us to detect and track a dim point target with

$S(C+N)R=0.01$. Green squares show instantaneous target detection in each frame most of which are false and the red line depicts the target track.

Figure 4 shows similar results for the LEO scenario with the parameters: Perigee=200 km, Apogee=400 km, Long of Ascending Node=6.26 rad, Argument of Perigee=0, Inclination=0.02 rad, FOV=0.02 rad.

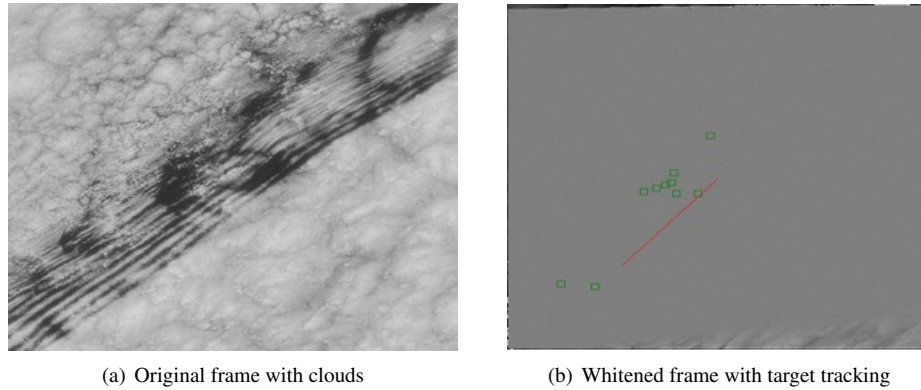


Figure 3. The results of clutter suppression and target tracking for a difficult non-stationary scenario (HEO MeteoSat data) using the CLUR algorithm with perspective prediction (red line – target track, green boxes – blips).

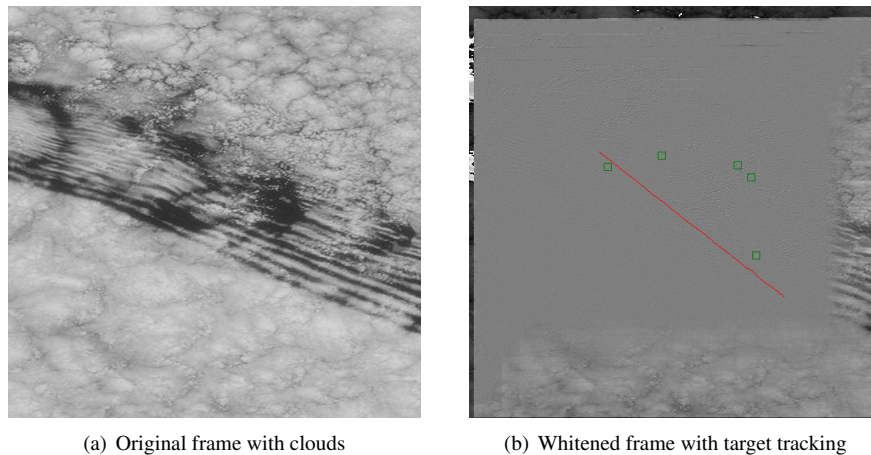


Figure 4. The results of clutter suppression and target tracking for a difficult non-stationary scenario (LEO data) using the CLUR algorithm with perspective prediction (red line – target track, green boxes – blips).

4. NONLINEAR FILTERING BASED TRACK BEFORE DETECT ALGORITHMS

In classical tracking methods, a thresholding operation is performed on the detection metric (e.g., based on intensity or frame differences) formed in individual scans/frames of data to generate target detections that are subsequently processed by data association and state estimation algorithms. Thresholding, however, causes partial loss of information, and target tracking based on this approach may be completely infeasible in situations with severe clutter and/or noise (if the detection threshold is set low enough to detect very dim targets, the number of clutter detections may result in either poor track estimation performance, or may prohibit real-time operation as the number of data association hypotheses explodes). In track-before-detect, information from individual frames is integrated over time until the number and locations of targets can be accurately estimated [2, 6, 7]. In our approach to track-before-detect, clutter-suppressed frames are used to update a non-parametric statistical background scene model that is built up on-the-fly to account for intensity variations due to effects such as noise and clutter leakage. Each clutter-suppressed frame is evaluated in the

statistical model to estimate the probability that the intensity of each optical sample has been modified by the presence of a moving target. The moving target probabilities are then integrated over time, based on probabilistic constraints on possible target motions, to develop the *a posteriori* probability distribution function over the space of possible target locations, based on the measurement history and any available *a priori* information (note that this *a priori* information is not a requirement). A track can be initiated by an external cue, such as a track formed from another sensor processor, or initiated automatically by our multiple target hypothesis management algorithm. In the latter case, detections/tracks are declared and reported when likelihoods of hypothesized target trajectories become sufficiently large. Subsequently, the track state estimates are updated with information from each new data scan as it becomes available.

Estimation of the posterior probability over the space of possible target trajectories is complicated by the nonlinearities in target dynamics and optical measurement (which involves a highly nonlinear projective function). To meet this challenge, we employ particle filtering methods—in particular, the sampling-importance-resampling (SIR) filter, for modeling and updating the posterior distribution [8]. Particle filters are well-suited for this problem since they are essentially non-parametric density estimators, and there is no constraint on the underlying structure of the probability density function (PDF). In contrast, state estimation problems in which nonlinear dynamic models, nonlinear measurement models, or non-Gaussian noise processes are present pose fundamental difficulties when applying standard Kalman filtering techniques based on linearization. Particle filtering algorithms do not require linearization of dynamic equations or measurement equations. Updating the target state PDF simply requires values of the measurement likelihood function evaluated at discrete points in the state space. In our algorithm, the likelihoods are obtained from evaluating each clutter-suppressed optical sample in the statistical background model, as previously described. In the case of tracking in 3D coordinates, we apply the sensor measurement model to project the 3D target position hypothesis for each particle into the image plane, prior to likelihood updating. For propagation through the state dynamic model, each particle is simply substituted into the dynamic equation and, with the simulation of any process noise variables, a new particle results.

As shown in the example in Figure 5, after multiple frames the particle distribution converges such that clusters of particles are located in the most likely regions of the state space, with a small fraction of the particles distributed more diffusely. As a result, we have found that our particle filter-based track-before-detect algorithm is more than two orders of magnitude more efficient (in terms of computation and storage requirements) compared with the classical 3D velocity-matched filter [7], for the same level (near-optimal effective SNR increase) of performance. This is true even though the particle filter was configured to account for possibly large target maneuver accelerations. Notably, our current C++ implementation of particle filtering-based track-before-detect is able to process MSX SBV data in near-real-time. The explanation for the efficiency gain in the recursive particle filter algorithm is that after processing each frame of data, during the particle re-sampling step, the particles are automatically re-allocated to perform more finely-spaced searches for target locations and velocities in regions of the state space that are found to be most likely (based on processing multiple past frames of data), whereas in the 3D velocity-matched filter, hypotheses are allocated uniformly while processing the entire batch of frames.

In Figure 5, we provide an example of track-before-detect using MSX SBV data. This example is interesting because it contains two resident space objects (RSOs), one which is blurred by rapid motion of approximately 30 pixels/frame, and the other, which is much dimmer, moves at only approximately 1/3 pixel/frame. This requires a very diffuse distribution of particle velocities, and fairly large process noise power spectral density in the target dynamics model. Furthermore, it is important to be able to track both the dim (mean intensity of 3) and bright (mean intensity of 19) targets simultaneously, which is possible using our statistical background modeling algorithm, which accurately recognizes both low- and high-intensity moving targets as anomalies, compared with the background scene. In Fig. 5(a), the fifth frame in the sequence is shown (the square root of the intensities are plotted to provide improved contrast). In Fig. 5(b), the initial uniform distribution of particle locations is shown (in this example, a 2D linear velocity white noise acceleration target dynamics model was used), with lighter intensities denoting larger numbers of particles within an optical resolution cell. In Fig. 5(c), the target probabilities produced by evaluating the fifth frame in the statistical background model are shown, with lighter intensities denoting higher probabilities. Finally, in Fig. 5(d), the particle distribution after processing the fifth frame is shown, and cues are provided to the locations of both targets, which have been automatically detected (after 3 and 5 frames for the brighter and dimmer targets, respectively).

In Figure 6, we provide an example of track-before-detect in 3D coordinates. The frame sequence was generated synthetically using measured EUMETSAT clutter, but with simulated target trajectories and intensities ($SCR = 1/1000$) and additive white Gaussian sensor noise ($SNR = 1/6$). As shown in this example, tracking in 3D physical world coordinates using a single optical sensor is possible in some cases (e.g., non-nadir viewing of a ballistic trajectory with a known launch point), and when ambiguity does exist, it is well-represented in the particle filter. In this example,

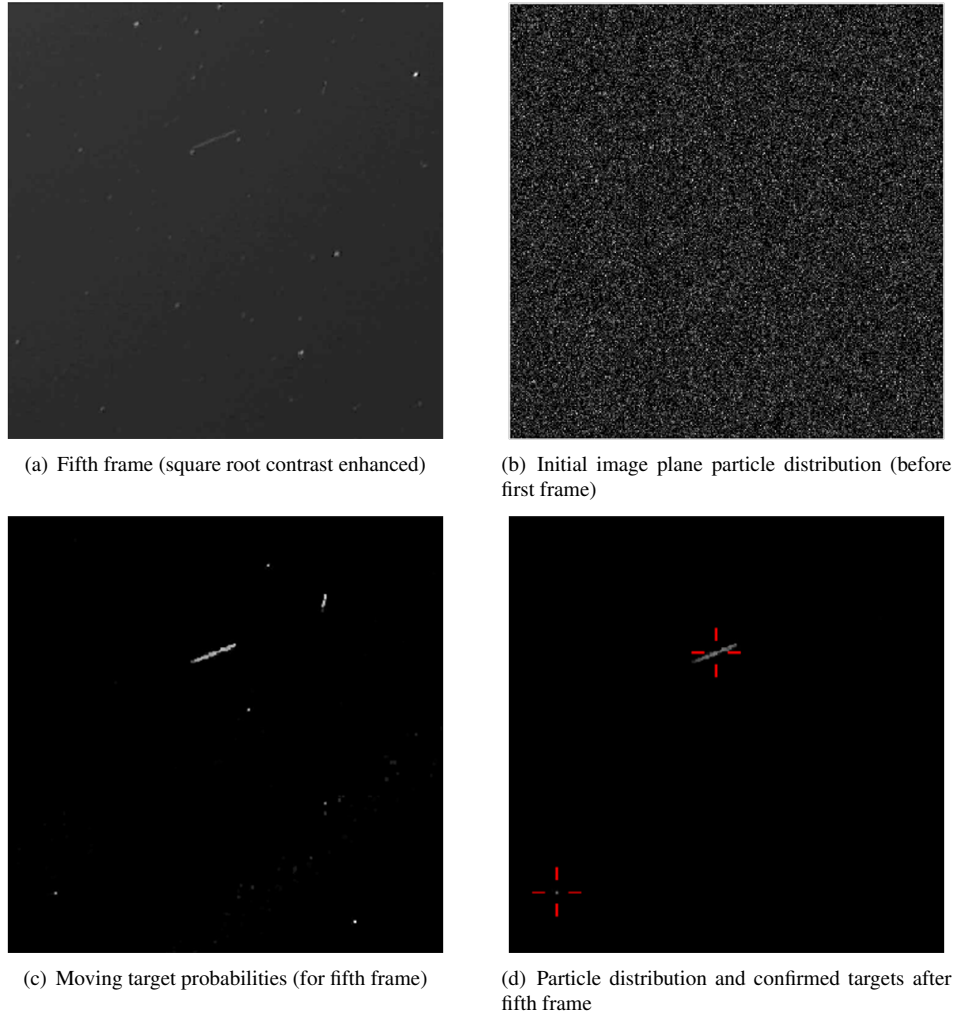
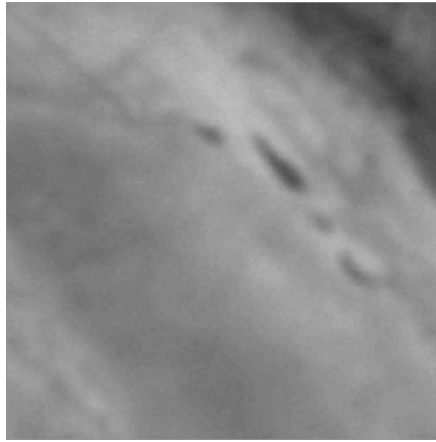


Figure 5. Track-before-detect results in MSX SBV for two RSOs (one extremely dim) with velocities and intensities differing by factors of 100 and 6, respectively.

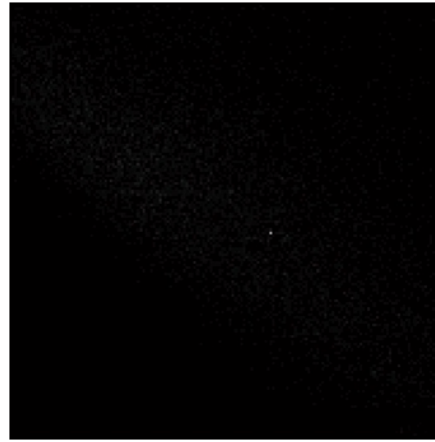
we assumed that the launch location and time were known (e.g., from bright plume detection), and that an initial estimate of the missile launch heading and elevation angles was available. The angle estimates were assumed to be very inaccurate, such that the initial uncertainty on the impact point location was very large: 1,500 km 3-sigma uncertainty, for a trajectory length of 1,500 km. In Fig. 6(b), the particle distribution is shown after processing 50 frames at a rate of 1 Hz, and the presence of a single target is clearly seen in the peaked distribution. The target has been automatically confirmed by the algorithm before this time, although visual cueing was not used in this experiment. In general, tracking in 3D provides improved estimation accuracy, and enables improved multi-sensor fusion and trajectory prediction, and as shown here, when combined with sensor motion compensation and spatial-temporal clutter suppression, this processing can be applied even for dim targets against terrestrial and other highly cluttered backgrounds.

5. CONCLUSIONS

In this paper, we have shown the need for and effectiveness of data-driven registration processing, spatial-temporal clutter estimation and rejection, and nonlinear stochastic track-before-detect processing for low observable targets against cluttered terrestrial, earth-limb, and celestial backgrounds. Notably, we have demonstrated that for some real-world applications it is currently feasible to perform this processing in near-real-time using a desktop PC. Furthermore,



(a) Simulated frame with EUMETSAT background clutter



(b) Projection of 3D particles into image plane

Figure 6. Projection of 3D particles (after 50 sec.) into the image plane for a simulated target against EUMETSAT background clutter (SCR = 1/1000) with simulated sensor noise (SNR = 1/6).

we expect that the developed algorithms have utility in a wide range of current and future systems being developed for space-based EO and IR surveillance.

ACKNOWLEDGEMENTS

The work of Alexander Tartakovsky was supported in part by the Missile Defense Agency contract W91260-08-C-0004 at Argo Science Corp., as well as by the U.S. Army Research Office MURI grant W911NF-06-1-0094, and by the U.S. National Science Foundation grant CCF-0830419 at the University of Southern California. The work of Andrew Brown was supported in part by the Missile Defense Agency contract W91260-08-C-0004 at Toyon Research Corporation. The work of James Brown was supported by the Air Force.

REFERENCES

- [1] Bar-Shalom, Y. and Li, X.R. *Estimation and Tracking: Principles, Techniques and Software*, Artech House, Boston-London, 1993.
- [2] Kligys, S., Rozovsky, B. L., and Tartakovsky, A. G., Detection Algorithms and Track Before Detect Architecture Based on Nonlinear Filtering for Infrared Search and Track Systems, *Technical Report # CAMS-98.9.1, Center for Applied Mathematical Sciences, University of Southern California*, 1998. (Available at <http://www.usc.edu/dept/LAS/CAMS/usr/facmemb/tartakov/preprints.html>).
- [3] Tartakovsky, A. G., Asymptotic Performance of a Multichart CUSUM Test Under False Alarm Probability Constraint, *Proceedings of 44th IEEE Conference on Decision and Control and European Control Conference (CDC-ECC'05)*, December 12-15, 2005, pp. 320-325, Seville, Spain, Omnipress CD-ROM, ISBN 0-7803-9568-9.
- [4] Tartakovsky, A. G. and Brown, J., Adaptive Spatial Temporal Filtering Methods for Clutter Removal and Target Tracking, *IEEE Aerospace and Electronic Systems*, Vol. 44, No. 4, pp. 1522-1537.
- [5] Tartakovsky, A., Kligys, S., and Petrov, A., Adaptive Sequential Algorithms for Detecting Targets in Heavy IR Clutter, *SPIE Proceedings: Signal and Data Processing of Small Targets*, (O.E. Drummond, Ed.), Vol. 3809, pp. 119-130, Denver, 1999.
- [6] Ristic, B., Arulampalam, S., and Gordon, N. *Beyond the Kalman Filter-Particle Filters for Tracking Applications*, Artech House, 2004.
- [7] Reed, I., Gagliardi, R., and Stotts, L., Optical Moving Target Detection with 3-D Matched Filtering, *IEEE Transactions on Aerospace and Electronic Systems*, Vol. 24, No. 4, 1988.
- [8] Arulampalam, M. S., Maskell, S., Gordon, N., and Clapp, T., A Tutorial on Particle Filters for Online Nonlinear/Non-Gaussian Bayesian Tracking, *IEEE Transactions on Signal Processing*, Vol. 50, No. 2, 2002.